Vol.3 Nol. 1,2
Winter&Spring 1992



# AXIAL FLOW IN A ROTATIONAL COAXIAL RHEOMETER SYSTEM II: HERSCHEL BULKLEY MODEL

S. H. Javadpour and S. N. Bhattacharya

*Chemical Engineering Division and Rheology and Materials Processing Centre, Royal Melbourne Institute of Technology, Melbourne, Victoria, Australia*

**Abstract**

Following recent works of several authors like Huilgol, Bhattacharya *et al.* and Javadpour *et al.*, this paper is to contribute further to the literature of axial flow in a rotational coaxial rheometer. We consider axial flow of Herschel Bulkley model between two concentric cylinders with the inner one rotating, while the outer cylinder is held stationary. An attempt has been made to direct the analysis toward an examination of the relationship between moment (M) and angular velocity ($\Omega$) at the inner cylinder. The radial dependence of the shear stress and viscosity follows directly by our mathematical analysis with a simple numerical procedure. We describe the relationship between shear stress and shear rate and the dependence of these on axial flow rate in the annular region, for power law and Herschel Bulkley fluids.

## Introduction

Helical flow is generated by rotating one or both of two concentric cylinders while simultaneously imposing an axial pressure gradient upon the fluid in the annular space. We are concerned only with the case where the outer cylinder is stationary and the inner cylinder rotates with angular velocity $\Omega$ . It can be shown from the equation of motion that the stress field, regardless of the fluid rheology is given by

$$\tau_{r\theta} = \frac{M}{2\pi r^2}$$

where M is the torque per unit length. The annular gap between the inner and outer cylinders is kept small in comparison to the diameter of the cup or the bob in order to reduce the secondary flow within the annular space.

Theoretical analysis for helical flow was first considered by Rivlin [1]. Subsequently, several authors have studied the problem of the helical flow of general fluid making no special constitutive assumptions other than incompressibility [2-5]. Rivlin presented his results in terms of eight material functions. Noll and Coleman showed that only three are necessary. Fredrickson [6] has derived a solution for the combined axial and tangential flow for an arbitrary, inelastic, non-Newtonian fluid in an anulus. His equations are actually a solution to a special case of the system of differential equations derived by Rivlin [1]. He has also shown how his equations could be generalized to give the solution of the problem posed by Rivlin. Both Coleman and Noll [4] and Fredrickson [6] concluded that the helical flow of any fluid may be characterized by two parameters, the angular velocity and the shear stress-shear rate, which are dependent upon the axial pressure gradient. Dierckes *et al.* [7] have presented an analytical solution of the rotating outer cylinder, for power law fluid ending with

**Keywords:** Helical flow, Herschel Bulkley fluid, Power law fluid, Rheology

two non-linear differential equations for the components of velocity. These equations which are complicated and required numerical solution retained the axial pressure gradient term as one of the variable parameters. Specific helical flows have been studied experimentally by some authors [7,8]. Tanner [9] presented the theory of helical flow as applied to a model due to Oldroyd [10] along with some experimental results. Savins *et al.* [11] have presented a quantitative prediction to show how the axial discharge rate and pressure gradient and angular velocity and torque become coupled when a fluid exhibiting a shear-dependent viscosity behaviour is subjected to a helical flow field. They presented a numerical solution for an Oldroyd type of constitutive equation. They mentioned that the most interesting consequence of the coupling effect was that the axial flow resistance was lowered in a helical flow. Bird *et al.* [12] produced an analytical solution of the equation for the special case of narrow gap between the coaxial cylinders for special case of power law fluid i.e. n = 1/3. Huilgol proposed a trial and error method to solve the helical flow for general fluids in terms of four parameters including one related to pressure drop along the axial flow [13]. Bhattacharya *et al.* [14] solved the problem of axial flow in a rotational rheometer for power law fluids, along with some experimental results. In their analysis the axial pressure gradient term was eliminated; thereby reducing the number of variable parameters studied in this analysis. Following this study, Javadpour *et al.* [15] extended the analysis to that for helical flow of Bingham plastic fluid in an annular space. They were able to obtain the shear rate, shear stress and viscosity distribution for different values of flow rate, torque and yield stress.

In this paper, the axial flow of the Herschel-Bulkley model through the annulus between two concentric circular cylinders is studied.

## MATHEMATICAL MODEL

We consider the motion generated by a cylinder rotating (the bob) inside a fixed concentric cylindrical housing (the cup), with the velocity distribution referred to cylindrical polar co-ordinate of the form

$$v_z = v(r),\ v_r = 0,\ v_\theta = r\omega(r) \qquad (1)$$

which automatically satisfies the equation of continuity.

When $v=0$, we have a velocity distribution suitable for use in the problem of flow between rotating concentric cylinder, and when $\omega = 0$, we have a velocity field appropriate to steady flow through a pipe of circular cross section. An attempt has been made to direct the analysis toward an examination of the relationship between moment (M) and angular velocity ($\Omega$) and the dependence of this on the axial flow rate.

We express the gravitational force in terms of a scalar potential $\psi$ by

$$g = -\nabla\Psi \qquad (2)$$

and define

$$\Phi = P + \rho\Psi \qquad (3)$$

where $\rho$ is the fluid density (constant), P is the fluid pressure. Thus, the components of the equation of motion, written in terms of physical components of the stress tensor are

$$\frac{1}{r}\frac{d}{dr}(rt_{(rr)}) - \frac{1}{r}t_{(\theta\theta)} - \frac{\delta\Phi}{\delta r} = -\rho r\omega^2 \qquad (4)$$

$$\frac{1}{r}\frac{d}{dr}(rt_{(rz)}) - \frac{\delta\Phi}{\delta z} = 0 \qquad (5)$$

$$\frac{1}{r}\frac{d}{dr}(r^2 t_{(r\theta)}) - \frac{\delta\Phi}{\delta\theta} = 0 \qquad (6)$$

where $t_{(rr)}$, $t_{(r\theta)}$, $t_{(rz)}$, $t_{(\theta\theta)}$, are the usual components of the stress tensor.

In the present example, we obtain

$$t_{(rz)} = \frac{v'}{\xi}\tau(\xi);\quad t_{(r\theta)} = \frac{r\omega'}{\xi}\tau(\xi) \qquad (7)$$

where $\tau$, the shear stress, will depend on the total rate of shearing, $\xi$, given by

$$\xi = \sqrt{(v')^2 + (r\omega')^2} \qquad (8)$$

We know from (1) and our postulate of a simple fluid that the stress can only be a function of r. This leads to the conclusion that $\Phi$ can at most be of the form

$$\Phi = g(r) + 2\alpha_1 z + c_1\theta \qquad (9)$$

where $\alpha$ and $c_1$ are constants. Then integration of (5) and (6) results in

$$t_{(rz)} = \alpha r + \frac{1}{r}\beta \qquad (10)$$

$$t_{(r\theta)} = \frac{1}{2}c_1 + \frac{1}{r^2}c_2 \qquad (11)$$

where the constants are determined by application of suitable boundary conditions.

From a combination of (7) with (10) and (11) there results a pair of differential equations for the velocity components

$$\upsilon'_{(r)}=\left(\alpha r+\frac{\beta}{r}\right)\frac{\xi}{\tau(\xi)} \quad (12)$$

$$\omega'(r)=\left(\frac{1}{2r}c_1+\frac{c_2}{r^3}\right)\frac{\xi}{\tau(\xi)} \quad (13)$$

where from (8) one may write

$$\tau(\xi)=\left\{\left(\alpha r+\frac{\beta}{r}\right)^2+\left(\frac{C_1}{2}+\frac{C_2}{r^2}\right)^2\right\}^{\frac{1}{2}}=f(r) \quad (14)$$

$$\xi=\tau^{-1}(f(r)) \quad (15)$$

These relationships are well-documented in the literature [16].

Thus, in principle we can solve the velocity profile from (12) - (13) once the boundary conditions, and hence the values of $c_1$, $c_2$, $\alpha$, and $\beta$, are known. We see that the velocity field is completely determined, for a given set of boundary conditions, by the single material function $\tau(\xi)$.

The non-slip condition applied at the inner and outer cylinders yield the boundary conditions

$$\upsilon(R_1)=\upsilon(R_2)=0, \quad (16)$$

$$\omega(R_1)=\Omega, \qquad \omega(R_2)=0 \quad (17)$$

where $\Omega$ is the angular velocity of rotation of the inner cylinder.

## Analysis for the Herschel Bulkley Model

We now consider the situation for the flow of the Herchel Bulkley model, namely

$$\tau(\xi)=\delta_y+\kappa\xi^n \quad \text{and} \quad \eta(\xi)=\kappa\xi^{n-1}+\delta_y\xi^{-1} \quad (18)$$

where $\eta(\xi)$ is known as the shear-dependent viscosity or "apparent viscosity", $\delta_y$ is the yield stress, $\kappa$ is the consistency index, and n is the power law exponent.

Equations (12) and (13) then become

$$\left[\kappa(\upsilon'^2+r^2\omega'^2)^{\frac{n-1}{2}}+\delta_y(r^2\omega'^2+\upsilon'^2)^{-\frac{1}{2}}\right]\upsilon'(r)=\alpha r+\frac{\beta}{r} \quad (19)$$

$$\left[\kappa(\upsilon'^2+r^2\omega'^2)^{\frac{n-1}{2}}+\delta_y(r^2\omega'^2+\upsilon'^2)^{-\frac{1}{2}}\right]r\omega'(r)=-\frac{M}{2\pi r^2} \quad (20)$$

Equations (19), (20) together imply

$$\upsilon'(r)=-\frac{2\pi}{M}(\alpha r^2+\beta)\,r^2\omega' \quad (21)$$

Substituting equation (21) into (20) yields

$$\omega'=-\Gamma(r,\alpha,\beta)\left[\frac{Mr^{-3}}{2\pi\sqrt[n]{\kappa}\,\Gamma(r,\alpha,\beta)}+\delta_y\right]^{\frac{1}{n}} \quad (22)$$

where

$$\Gamma(r,\alpha,\beta)=\frac{1}{\sqrt[n]{\kappa}}\left[r\sqrt{1+\frac{4\pi^2r^2}{M^2}(\alpha r^2+\beta)^2}\right]^{-1} \quad (23)$$

and integration of (22) subject to the boundary conditions (17) gives

$$\Omega=\int_{R_1}^{R_2}\Gamma(r,\alpha,\beta)\left[\frac{Mr^{-3}}{2\pi\sqrt[n]{\kappa}\,\Gamma(r,\alpha,\beta)}+\delta_y\right]^{\frac{1}{n}}dr \quad (24)$$

an equation linking $\Omega$ and M through $\alpha$ and $\beta$.

Applying equation (22) to (21) and integrating subject to the condition (16) yields

$$G_1(\alpha,\beta)\equiv\int_{R_1}^{R_2}(\alpha r^2+\beta)r^2\Gamma(r,\alpha,\beta)\left[\frac{Mr^{-3}}{2\pi\sqrt[n]{\kappa}\,\Gamma(r,\alpha,\beta)}+\delta_y\right]^{\frac{1}{n}}dr=0 \quad (25)$$

However, there is a further constraint on the axial velocity $\upsilon(r)$ that arises from the incompressibility of the fluid i.e. the axial flow rate at any cross-section of the annulus is constant.

If Q is this constant rate, this implies the extra condition

$$Q=2\pi\int_{R_1}^{R_2}r\upsilon(r)\,dr \quad (26)$$

Integrating by parts using (16) we obtain

$$\pi\int_{R_1}^{R_2}r^2\upsilon'(r)dr+Q=0 \quad (27)$$

Equations (27), (21) and (22) together give

$$G_2(\alpha,\beta)=\int_{R_1}^{R_2}(\alpha r^2+\beta)r^4\Gamma(r,\alpha,\beta)\left[\frac{Mr^{-3}}{2\pi\sqrt[n]{\kappa}\,\Gamma(r,\alpha,\beta)}+\delta_y\right]^{\frac{1}{n}}dr+\frac{MQ}{2\pi^2}=0 \quad (28)$$

We may now regard the problem as one of finding $\alpha$ and $\beta$ from the simultaneous non-linear equations

$$G_1(\alpha,\beta)=G_2(\alpha,\beta)=0 \quad (29)$$

This will allow us to obtain the function, $\upsilon(r)$, $\omega(r)$ and hence the complete velocity field. More significantly for the present discussion $\alpha$ and $\beta$ may be substituted into (24) to establish a relationship linking $\Omega$ and M with Q appearing as a parameter, via equation (28).

There are two special cases of the above analysis that deserve particular comment. (i) For a power law (pseudoplastic) fluid $\delta_y = 0$ and $\kappa = m$, equations (26) and (27) become

$$G_1(\alpha, \beta) = \int_{R_1}^{R_2} r^{\left(1-\frac{2}{n}\right)} (\alpha r^2+\beta)\, \Phi\, (r, \alpha, \beta)\, dr = O \tag{30}$$

and

$$G_2(\alpha, \beta) = \int_{R_1}^{R_2} r^{\left(3-\frac{2}{n}\right)} (\alpha r^2+\beta)\Phi(r, \alpha, \beta)\, dr + \left[\frac{2\pi m}{M}\right]^{\frac{1}{n}} \frac{MQ}{2\pi^2} = 0 \tag{31}$$

where

$$\Phi(r, \alpha, \beta) = \left[\sqrt{1+\frac{4\pi^2 r^2}{M^2}(\alpha r^2+\beta)^2}\right]^{\frac{1}{n}-1} \tag{32}$$

respectively, providing a relationship of $\alpha$ and $\beta$ in terms of Q.

(ii) For a Bingham plastic fluid: n=1, $\kappa = \mu_p$

$$G_1(\alpha, \beta) = \frac{1}{\mu_p}\int_{R_1}^{R_2} (\alpha r^2+\beta) r^{-1} dr + \frac{2\pi}{M}\int_{R_1}^{R_2} (\alpha r^2+\beta) r^2 \psi\, (r, \alpha, \beta)\, dr = 0 \tag{33}$$

and

$$G_2(\alpha, \beta) = \frac{M}{2\pi\mu_p}\int_{R_1}^{R_2} (\alpha r^2+\beta) r\, dr + \int_{R_1}^{R_2} (\alpha r^2+\beta) r^4 \psi\, (r, \alpha, \beta)\, dr + \frac{MQ}{2\pi^2} = 0 \tag{34}$$

where

$$\psi\, (r, \alpha, \beta) = \frac{\delta_y}{\mu_p}\left[r\sqrt{1+\frac{4\pi^2}{M^2} r^2 (\alpha r^2+\beta)^2}\right]^{-1} \tag{35}$$

## Estimation of Shear Stress and Viscosity

Calculations were performed for the Herschel Bulkley model using the same definition for total shear stress, fluidity and approximate viscosity [15].

In the present case fluidity is

$$\phi(\tau) = \left(\frac{1}{\kappa}\right)^{\frac{1}{n}} |\tau - \delta_y|^{\frac{1}{n}} |\tau|^{(1-n)} \tag{36}$$

and the total shear stress in the z-θ plane is defined as

$$\tau = \sqrt{\tau_{(r\theta)}^2 + \tau_{(rz)}^2} \tag{37}$$

Based on the total rate of shear $\zeta$ given by (8), viscosity may be obtained as total shear stress divided by the total shear rate, i. e.

$$\eta = \frac{\sqrt{\tau_{(r\theta)}^2 + \tau_{(rz)}^2}}{\sqrt{\upsilon'^2 + (r\omega')^2}} \tag{38}$$

and approximate viscosity is

$$\eta_{app.} = \kappa \xi_{app.}^{n-1} + \delta_y \xi_{app.}^{-1} \tag{39}$$

where

$$\xi_{app.} = \sqrt{\left(\frac{\Omega R_1}{R_2 - R_1}\right)^2 + \left(\frac{4Q}{(R_2^2 - R_1^2)(R_2 - R_1)}\right)^2} \tag{40}$$

## Numerical Solution

The value of $\alpha$ and $\beta$ from equation (29) calculated by the same procedure as described previously [15], results of comparison between viscosity and approximate viscosity are given at the different radial points in the annular region.

We also applied the value of $\alpha$ and $\beta$ to examine the relationship between shear rate and shear stress and the dependence of these on axial flow rate at different radial points in the annular region, for different values of torque.

## Results and Discussion

Theoretical results of shear stress, shear rate, viscosity and velocity profile for the Herschel Bulkley and power law fluids flowing through the annular region of a rotational rheometer are presented here. The assumed values of the diameters of the inner and outer cylinders of the rheometer have been arbitrarily taken as 0.0215m and 0.0242m respectively for the calculation; however, they correspond to the dimension of the rheometer which is

used in this laboratory for the experimental study. Values of n, $\kappa$ and $\delta_y$ have also been arbitrarily chosen covering a range of values.

Figures 1-3 present the relationship between total shear stress and total shear rates for power law fluids for three flow rates of $1x10^{-6}$, $1x10^{-5}$, and $1x\ 10^{-4}$, $m^3/s$ respectively. In Figure 1, the relationship is shown for a fluid of n equal to 0.729 and $\kappa$ equal to 0.482 Pa $s^n$. It is seen that the axial flow rate does not have any effect on the shear stress-shear rate relation. Estimates of shear stress-shear rate relation for other values of n and $\kappa$ such as 0.696 and 2.020 Pa $s^n$ and 0.85 and 10 Pa $s^n$ respectively are shown in Figures 2 and 3. For all these fluids the axial flow rate did not have any effect on the total shear stress.

Some variation was however observed when the component of the stress tensor, $\tau_{r\theta}$, i.e. the shear stress in the $\theta$ direction (termed as shear stress), was calculated as a function of shear rate ($r\omega'$). It should be noted that this is the shear stress which is measured by the rotating bob of a concentric rotational rheometer. For n equal to 0.6 and $\kappa$ equal 10 Pa $s^n$, the shear stress was found to decrease slightly with increase in axial velocity (Figure 4). A smaller decrease was observed for a lower value of

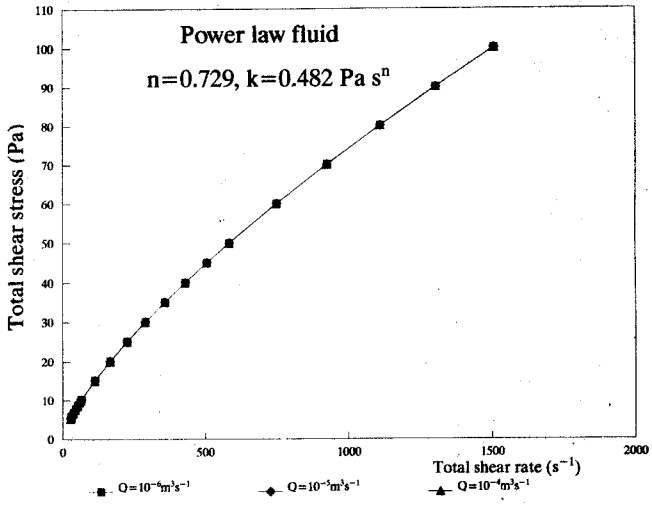


**Figure 1.** Effects of axial flow on shear stress-shear rate relation.

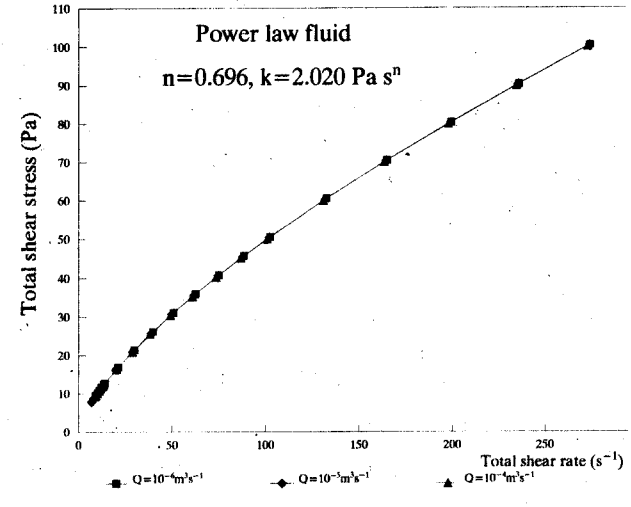


**Figure 2.** Effects of axial flow on shear stress-shear rate relation.

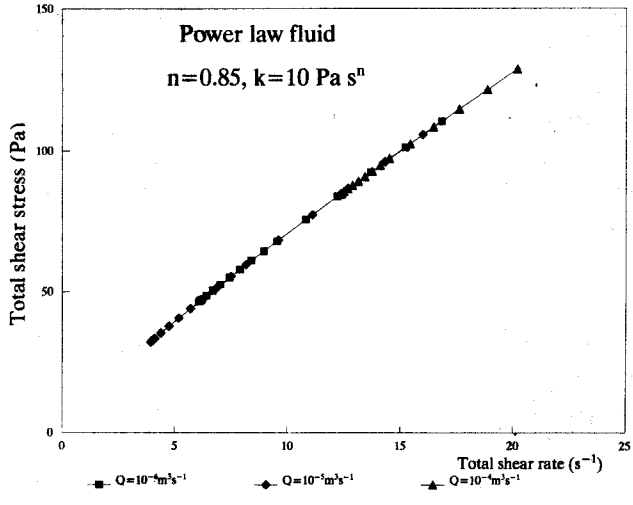


**Figure 3.** Effects of axial flow on shear stress-shear rate relation.

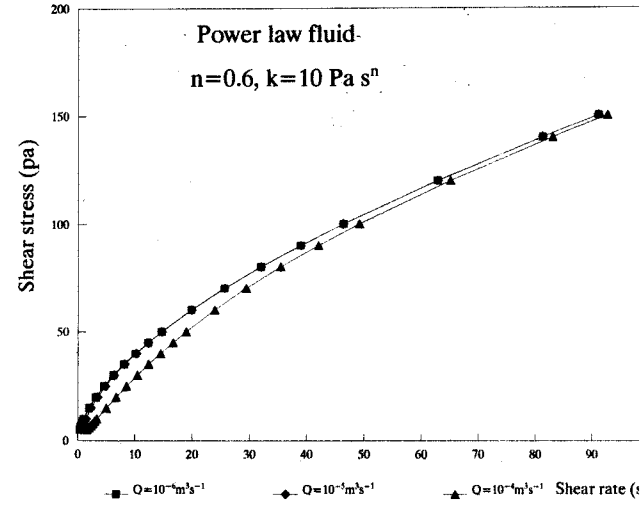


**Figure 4.** Effects of axial flow on shear stress-shear rate relation.

κ such as 2.02 Pa $s^n$ as shown in Figure 5.

Total shear stress versus total shear rate data for two Herschel Bulkley fluids as a function of axial flow rate are presented in Figures 6 and 7 respectively. Here also no variation in shear stress is observed for change in axial flow rate.

Figure 8 shows the effect of axial flow rate on shear stress. It may be noted from this figure that there is a noticeable decrease in shear stress with increase in axial flow rate. Similar behaviour was noted by Savins and Wallick [11] when they analysed the helical flow using an Oldroyd type constitutive equation. They observed that with increase in helical flow the viscosity values decreased at any radial position in the annulus. Although their analysis was based on the application of a given applied axial pressure gradient, it was demonstrated that the axial discharge rate increased under a helical flow condition in comparison to a simple annular flow. The magnitude of increase in axial flow rate under a given applied pressure gradient was found to be dependent on the values of the fluid model parameters. In our analysis it has been similarly observed that the axial velocity produces greater decrease in viscosity when the value of κ is increased from 10 Pa $s^n$ to 25 Pa $s^n$ (Figure 9). A

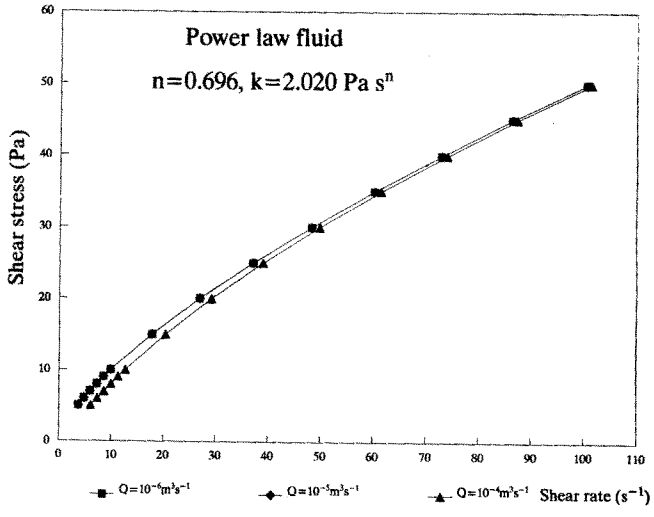


**Figure 5.** Effects of axial flow on shear stress-shear rate relation.

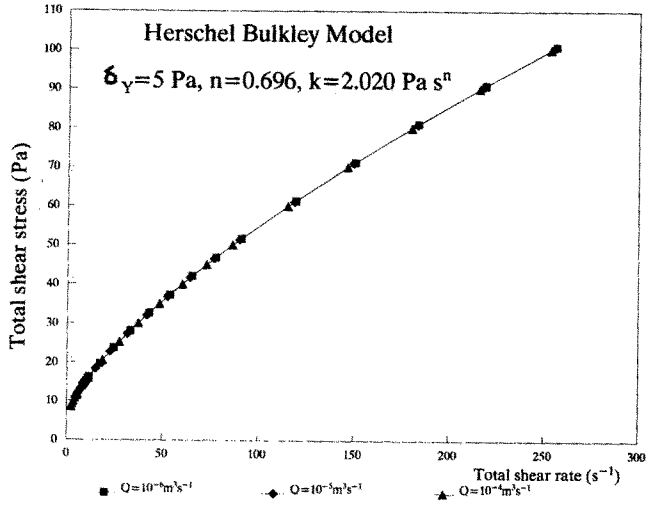


**Figure 6.** Effects of axial flow on shear stress-shear rate relation.

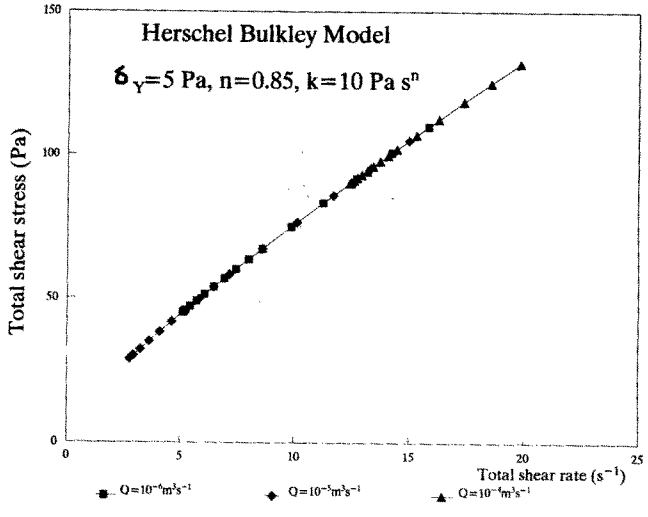


**Figure 7.** Effects of axial flow on shear stress-shear rate relation.

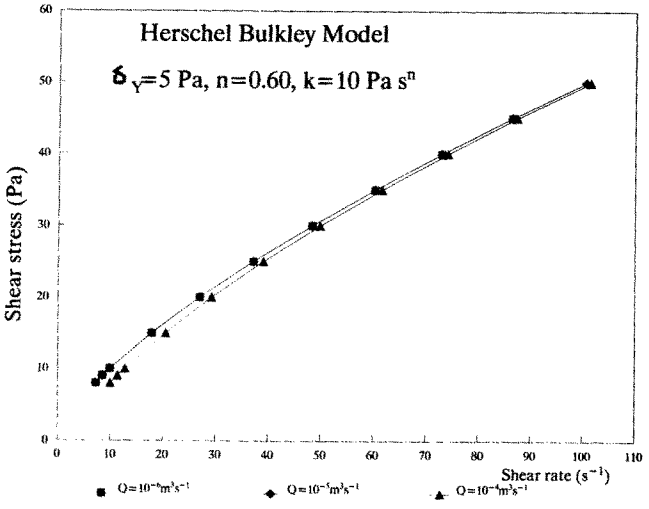


**Figure 8.** Effects of axial flow on shear stress-shear rate relation.

comparison between Figures 8 and 9 shows that for axial flow varying from $10^{-6}$ to $10^{-4}$ $m^3/s$, the percentage drop in shear stress for a shear rate of 32 $s^{-1}$ is 3.5 in Figure 8, and 7.5 in Figure 9. This indicates that the degree of viscosity reduction is higher for a fluid having a higher value of $\kappa$.

An approximate value of the viscosity has been calculated using equation (39). This prediction is simple and may be compared with the rigorous prediction that may be obtained from the ratio of shear stress to shear rate data as presented in Figures 1 to 7. The rigorous viscosity data calculated from Figure 2 is compared with the corresponding approximate data in Figure 10 for a power law fluid. It is seen that the approximate viscosity is higher than the true viscosity. However, the difference between the true and the approximate value somewhat diminishes at higher shear rates. This behaviour is however pronounced for a Herschel Bulkley fluid as shown in Figure 11. Here for an axial flow rate of $10^{-6}$ $m^3/s$ the difference between the true and the approximate viscosity disappears at higher shear rate.

The velocity profile in the annular region may be estimated if equation (21) is integrated as a function of r. Figure 12 shows the velocity profile for power law

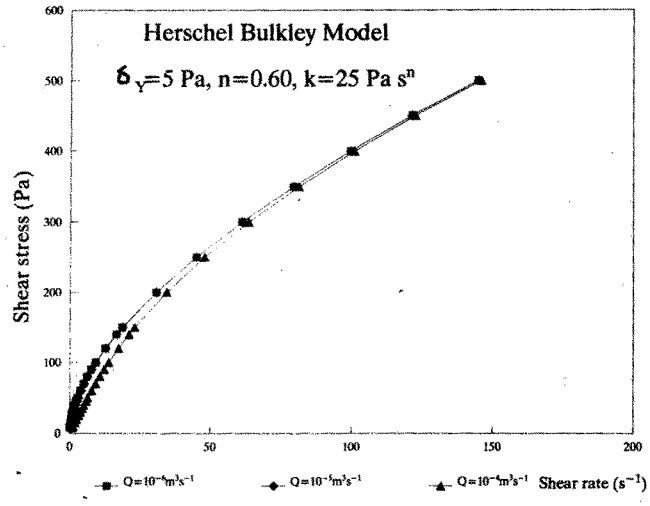


**Figure 9.** Effects of axial flow on shear stress-shear rate relation.

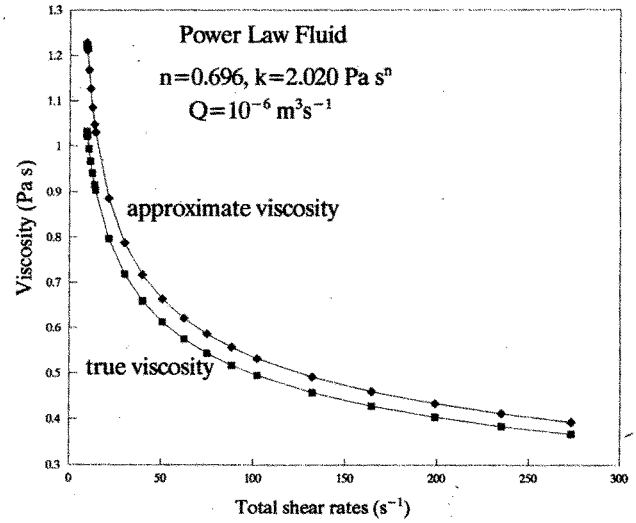


**Figure 10.** Comparison between true and approximate viscosity at $R_1$ =0.0215m.

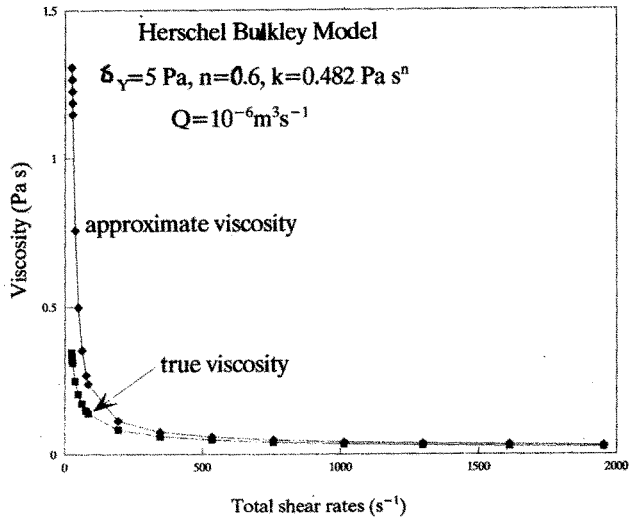


**Figure 11.** Comparison between true and approximate viscosity at $R_1$ =0.0215m.

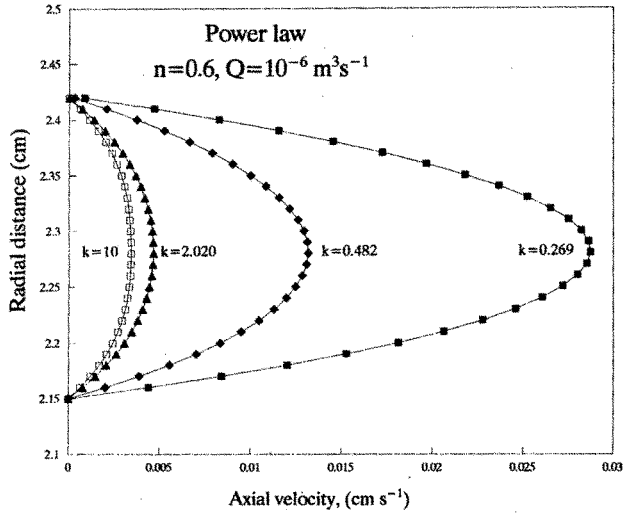


**Figure 12.** Effect of consistency on velocity profile.
Note: k is in $Pas^n$

fluids of n equal to 0.6 and κ of different values for an axial flow of $10^{-6}$ $m^3/s$. The profile becomes flatter with decreasing maximum velocity as the value of κ increases. Similar behaviour is observed for the Herschel Bulkley fluids. A comparison between the velocity profiles of a power law and a Herschel Bulkley fluid is

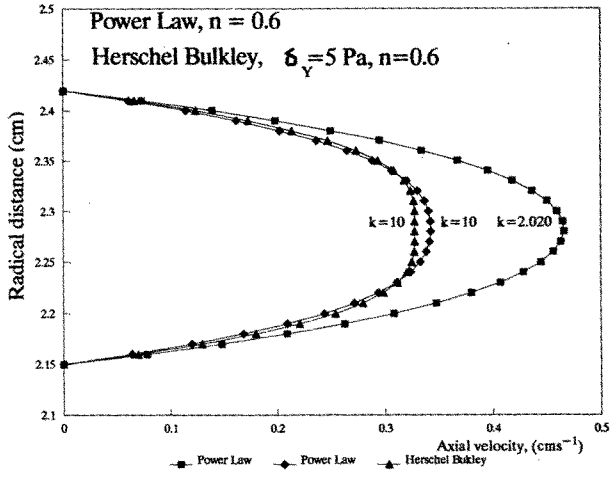


**Figure 13.** Effect of consistency on velocity profile. Note: k is in $Pas^n$.

presented in Figure 13, where the values of κ have been varied. It may be noted from Figure 13 that the difference between the velocity profile for power law and Herschel Bulkley fluids almost disappears when κ becomes high and $\delta_y$ is low. For a power law fluid with a high value of κ, such as 10 $Pas^n$, the velocity profile is similar to that of a Herschel Bulkley fluid with the same n and κ. However, the central region of the annulus for the Herschel Bulkley fluid has a region of constant velocity as is expected of a yield stress fluid.

## Acknowledgement

Dr. Javadpour extends his sincere appreciation for the financial support given to him by the Ministry of Science and Higher Education in Iran, and for the hospitality of RMIT in Australia.

## References

1. R. S. Rivlin, *J. Rational Mech. Anal.*, **5**, 179 (1956).
2. W. Noll, *Arch. Rational Mech. Anal.*, **2**, 197 (1958).
3. B. D. Coleman, W. Noll, *ibid.*, **3**, 289 (1959).
4. B. D. Coleman, W. Noll, *J. Applied Phys.*, **30**, 10, p. 1508 (1959).
5. R. B. Bird, C. F. Curtiss, *Chem. Eng. Sci.*, **11**, 108 (1959).
6. A. G. Fredrickson, *ibid.*, **11**, 252 (1960).
7. A. C. Dierckes, W. Schowalter, *Ind. Eng. Chem. Fund.* **5**, 263 (1966).
8. D. R. Rea, W. Schowalter, *Trans. Soc. Rheol.* **11**, 125 (1967).
9. R. I. Tanner. Rheo. Acta, 3, Part I, 21; Part II, 26 (1963).
10. J. G. Oldroyd, Proc. Roy. Soc., A245, 278 (1958).
11. J. G. Savins, G. C. Wallick, J. A. I. Ch. E., 12, 357, (1966).
12. R. B. Bird, R. C. Armstrong, O. Hassager, "Dynamics of Polymeric Liquids" vol. 1, John Wiley & Sons (1987).
13. R. R. Huilgol, 5th National Conf. Rheo., Melbourne, 43 (1990).
14. S. N. Bhattacharya, A. Chryss, H. J. Connell and J. J. Shepherd, 5th National Conf. Rheo., Melbourne, 15 (1990).
15. S. H. Javadpour, S. Bhattacharya, *J. Sci. I. R. Iran* (Submitted).
16. W. R. Schowalter, Mechanics of Non-Newtonian Fluids (1978).